ATLAS NOTE

ATL-PHYS-PUB-2008-000

June 6, 2008

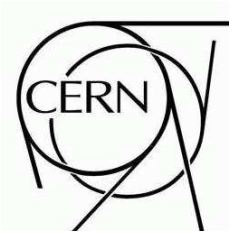

ATL-PHYS-CONF-2008-016

19 June 2008

High p_T Hadronic Top Quark Identification Part II: the lifetime signature

M. Vos

IFIC (U. Valencia/CSIC), Valencia, Spain

Abstract

At the LHC top quarks will for the first time be produced abundantly and with very large transverse momenta. For hadronic decays of top quarks at large p_T the three jets merge into a single jet: a top *monojet*. Identification of these objects among the overwhelming QCD di-jet background requires the development of specific experimental techniques. In this note the use of flavour tagging algorithms based on the B-hadron lifetime for the identification of top *monojets* will be explored.

1 Introduction

Highly boosted top quarks offer an interesting window on new physics. As the heaviest known particle, the top quark may play a crucial role in electroweak symmetry breaking. Many models predict heavy particles that decay preferentially into top quarks. Several recent papers have emphasised this point. Kaluza-Klein excited states of the gluon in Randall-Sundrum models couple strongly to the top quark [1]. A second example is a class of models where heavy counterparts to Standard Model particles of the same statistics lead to a cancellation of the radiative corrections to the Higgs mass. Examples of implementations are the Little(st) Higgs [2] and twin Higgs models [3].

Several ATLAS studies have investigated the potential for discovery of heavy resonances decaying into $t\bar{t}$ pairs [3, 4] for the models mentioned above. High p_T top quarks may also be produced in the decay of a heavy charged gauge boson. The decay $W_H \rightarrow tb$ has been studied in the context of little(st) Higgs [5] and LR Twin Higgs models [6].

At the LHC heavily boosted top quarks will be produced abundantly through Standard Model $t\bar{t}$ pair production. While at the Tevatron $t\bar{t}$ pairs are produced essentially at rest, at the LHC - with a center-of-mass energy of 14 TeV - top quarks are no longer heavy objects. The NLO cross-section for Standard Model $t\bar{t}$ pair production, where at least one of the top quarks has a transverse momentum $p_T > 200$ GeV is approximately 150 pb [1)].

The top quark decays into a W-boson and a b-quark with nearly 100 % branching ratio. Several authors [1] have pointed out the experimental challenge of top quarks with large transverse momenta, where the decay products are highly collimated. For hadronic decay of the W (nearly 70 % of cases) three jets will be found in a narrow cone. For large top quark transverse momenta, the separation between the three jets becomes so small that the individual decay products can no longer be distinguished by the standard jet reconstruction algorithms. At high p_T top quark are thus increasingly reconstructed as a single jet: a *monojet*.

In figure 1 this effect is represented in a more quantitative fashion. Jets are reconstructed in the vicinity of the top quark using the cone algorithm with an opening angle $\Delta R = \sqrt{(\Delta\phi)^2 + (\Delta\eta)^2} < 0.4$. For these jets, the fraction of cases is indicated where the W-boson (continuous line) or b-quark (dashed line) are within a distance $\Delta R < 0.4$ of the reconstructed jet direction. For practical purposes a top *monojet* topology is defined as those jets where both the W-boson and the b-quark are contained inside the jet cone. As expected, the probability for this to occur is a steadily rising function of top transverse momentum.

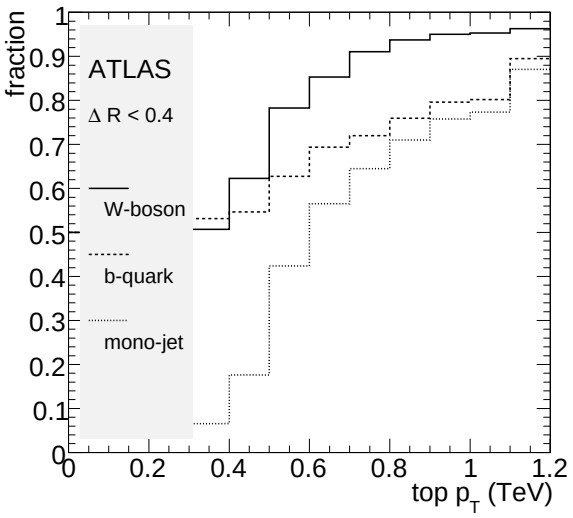

Figure 1: The fraction of top quark decays where the W-boson (continuous line) or b-quark (dashed line) are within $\Delta R = \sqrt{(\Delta\phi)^2 + (\Delta\eta)^2} < 0.4$ of the reconstructed jet axis versus top quark transverse momentum.

The standard reconstruction strategy for top quarks requires all decay products to be reconstructed separately [8]. At large top quark transverse momenta ($p_T > 400$ GeV) the efficiency of this *resolved* approach rapidly decreases. At the same time the probability to reconstruct the top quark decay products

[1)] The number has been determined using the MC@NLO [7] generator using the CTEQ6L parton density function.

as a single jet increases. Experimental methods that identify the top *monojets* without explicitly resolving the individual decay products therefore form a natural complement to the existing top reconstruction algorithms.

The principal challenge to this alternative approach is the identification of top *monojets* among the overwhelming QCD di-jet background.

In a recent ATLAS note [9], the potential to tag top *monojets* using the substructure in the calorimeter energy depositions has been discussed. The invariant mass reconstructed from the four-momenta of all calorimeter clusters is found to yield a powerful discriminant. A second, complementary handle is found in the last splitting scale as given by the Y-splitter [10] algorithm.

An independent handle may be found in the lifetime signature of the B-hadron embedded in the top *monojet*. Flavour tagging methods based on the long lifetime of B-hadrons have since long proven to be a powerful experimental tool. The ATLAS collaboration has developed a suite of *b-tagging* algorithms based on the precise reconstruction of charged tracks in the inner detector. The identification of tracks with large impact parameter, in combination with algorithms that explicitly search to reconstruct the secondary B-decay vertex, allows efficient tagging of b-jets.

In this note the ATLAS lifetime-based flavour-tagging algorithms are applied to hadronic top *monojets*.

In section 2 the Monte Carlo samples used for this study are briefly described. The reconstruction of the events is outlined in section 3. The flavour-tagging algorithms are revisited in some detail in section 4. Special emphasis is placed on the flavour tagging performance in high p_T jets. In section 5 the results of a study of the tagging performance for top *monojets* on a set of benchmark samples are reported. In section 6 the potential of these algorithms to isolate highly boosted top quarks from the full QCD di-jet background is discussed. Finally, in section 7, the conclusions of this study are summarized.

2 Monte Carlo Samples

In the framework of the ATLAS Computing System Commissioning (CSC) exercise large samples of Monte Carlo events have been generated. The response of a realistic and detailed detector model is simulated in full detail using GEANT4. The geometry known as ATLAS-CSC-01-02-00 is used, which at the time of writing contained the most up-to-date description on the inner detector material.

The geometry ATLAS-CSC-01-02-00 incorporates large-scale misalignments of inner detector elements. However, events have been reconstructed taking into account all the generated misalignment constants, so that virtually no misalignment effects should be observed. The impact of realistic alignment scenarios is studied in reference [11].

To characterize the ATLAS tagging performance at high p_T three data sets were generated using PYTHIA:

- 6601: $Z_H(m = 2TeV) \rightarrow u\bar{u}$ (20000 events)
- 6602: $Z_H(m = 2TeV) \rightarrow c\bar{c}$ (20000 events)
- 6603: $Z_H(m = 2TeV) \rightarrow b\bar{b}$ (20000 events)

The mass of the heavy resonance Z_H was chosen so that the samples provide jets in the range 200 GeV - 1 TeV.

The statistics in the official data samples (5000 events) is insufficient for a detailed study of the tagging performance. Therefore, for each sample an additional set of 15000 events was generated using the official production tools and identical software versions for generation, simulation and reconstruction. These events were carefully validated against the official samples.

At a later stage the official data sets were complemented with a fourth sample:

- extra: $Z_H(m = 2TeV) \rightarrow t\bar{t}$ (20000 events)

The above-mentioned data samples provide a very useful benchmark for the heavy flavour tagging performance. For a realistic physics analysis of heavily boosted top quarks, however, the background is formed by QCD di-jet events. In the CSC production, PYTHIA was used to generate an inclusive QCD sample. The samples were subdivided in eight bins of parton p_T. For the kinematic range discussed in this note the following three samples are relevant:

- J5: $280 < p_T < 560$ GeV, $\sigma = 12.5$ nb
- J6: $560 < p_T < 1120$ GeV, $\sigma = 344$ pb
- J7: $1120 < p_T < 2240$ GeV, $\sigma = 5.3$ pb

3 Reconstruction Algorithms

The official ATLAS reconstruction package (ATHENA release 12.0.6) is used to reconstruct the events.

The jet reconstruction algorithm used for this analysis is the iterative cone algorithm that takes calorimeter towers with size $\Delta\eta \times \Delta\phi = 0.1 \times 0.1$ as input (the collection is labelled as Cone4H1Tower). A cone size of $\Delta R = 0.4$ is used throughout the note. A more detailed description of the ATLAS jet reconstruction algorithms is found in [12].

In each of these data sets, tracks were reconstructed using all three ATLAS tracking algorithms (the default *New Tracking*, *iPatRec* and *xKalman*). In the following only *iPatRec* tracks are used. Tracks are reconstructed using the default settings of these algorithms. Recent descriptions of the ATLAS tracking code is found in [13].

Tracks are associated to the jets on the basis of a simple ΔR criterion: all tracks within a cone centered on the jet axis are considered for b-tagging. The default ATLAS jet-track association cone size is $\Delta R = 0.4$. However, for the very collimated high p_T jets the optimal performance is found for smaller association cones. Therefore, a value of $\Delta R = 0.2$ will be used in the following.

ATLAS reconstruction software is in continuous evolution. In particular, the reconstruction of charged tracks in high p_T jets is an area where considerable progress may be expected. Improvements in the clustering of hits in the pixel detector are expected from the use of the Time-Over-Threshold information. Changes in the ambiguity resolving during the pattern recognition stage may lead to improved tracking efficiency. This study necessarily forms a *snapshot* in this development.

4 Flavour Tagging Algorithms

The ATLAS *b-tagging* algorithms and their performance are described in detail in reference [14]. Here, only a brief overview is given of two algorithms based on the lifetime of B-hadrons.

The first, most straightforward set of algorithms is based on the measurement of the impact parameter of charged tracks. A detailed description is found in reference [15]. In the 2D algorithm the transverse impact parameter - the distance of closest approach to the beam axis of the charged particle trajectory - is used. In the 3D algorithm the transverse impact parameter is combined with the longitudinal impact parameter.

The impact parameter significance is obtained by dividing the measurement by an estimate of the error as returned by the track fit (a parameterization is used to describe the hit errors). Finallly, the impact parameter significance is signed according to the projection of the impact parameter on the jet axis. The sign convention is chosen such that tracks stemming from the decay of particles with a long lifetime get assigned a positive sign. A likelihood is formed from the ratio of probabilities to find a

track with a given signed impact parameter significance in a b-jet or light jet. The output of the impact parameter based tagging algorithms is a jet likelihood that is the product of the likelihoods of all selected tracks in the jet.

A second, more involved, class of algorithms explicitly reconstructs the decay vertex of the B-hadron starting from the tracks in the jet [2)]. Detailed information may be found in [16]. Two flavour tagging algorithms based on secondary vertex reconstruction have been implemented [17, 18] in the standard ATLAS reconstruction software. Here, the *SV1* algorithm is studied. The presence of a reconstructed displaced vertex - after rejection of conversions and V^0 vertices - is a good indication for a heavy (b or c) quark. The tag is further refined by the use of observables like the invariant mass of the tracks associated to the vertex, the fraction of the jet energy carried by tracks associated to the vertex, the vertex multiplicity and (in one algorithm) the distance of the secondary vertex to the primary vertex. As in the case of the impact parameter based algorithms probability density functions of these observables are calculated and the algorithms return a combined likelihood.

To reach the best possible performance the impact parameter and secondary vertex based algorithms are combined. A combined likelihood is obtained by summing the likelihoods of the tagging algorithms, i.e. ignoring potential correlations between algorithms. In the following, the results of the combined *SV1+IP3D* algorithm will be reported.

The tagging algorithms rely heavily on the efficiency and purity of the input track collection. Therefore, the tracks associated to the jet are filtered with a set of requirements that includes cuts on the number of hits in the pixel detector and in the semi-conductor tracker, and maximum values for the transverse and longitudinal impact parameters.

The performance of the ATLAS track reconstruction algorithms for very high p_T jets has been studied in some detail in [14]. Pattern recognition in the dense core of these jets challenges the ATLAS inner detector and reconstruction software. Signals from close-by tracks may merge into a single hit. Hits shared between more than one track - a relatively rare phenomenon for low p_T jets - become much more frequent. Often, more than one compatible hit is found, leading to ambiguities in the hit assignment. The combined effect is a significant deterioration of the tracking efficiency and fake rate with respect to more benign environments. Moreover, the determination of the track parameters and error matrix becomes less reliable, leading to an increased probability for tracks from the primary vertex to *fake* late decays.

The optimal values of the flavour tagging algorithm parameters for very high p_T jets are found to deviate considerably from the low p_T optima:

- Tracks reconstructed using the iPatRec algorithm are found to yield better tagging performance than those returned by the ATLAS default algorithm.

- The typical transverse momenta of tracks from B/D decays are considerably larger when compared to tracks in low p_T jets. Moreover, problems due to imperfect pattern recognition tend to be most pronounced for low-momentum tracks, with large propagation errors due to multiple scattering. The minimum transverse momentum requirement is therefore set to 5 GeV, instead of the default value of 1 GeV.

- High p_T jet tracks from B/D-decay tend to be collimated in a very small region around the B-hadron direction (which can be roughly identified with the jet axis). Tracks from fragmentation - whose number increases significantly for high p_T jets - tend to spread out over a larger area. These tracks carry no information on the jet flavour and thus dilute the tagging performance. Therefore, a small association cone ($\Delta R = 0.2$) yields significantly better results for very high p_T jets than the default cone size ($\Delta R = 0.4$).

[2)] In many cases, a tertiary D-decay vertex is present, that may or may not be reconstructed separately.

- In the default algorithm tracks with one or more shared hits form a special category that has its own calibration. Hits shared between more than one track are far more frequent in high p_T jets. The allowed number of shared hits for the standard category is therefore increased to 3 (for the *SV1* algorithm) and to 3 in the pixel detector and 3 in the semi-conductor tracker (for the *IP3D* algorithm).

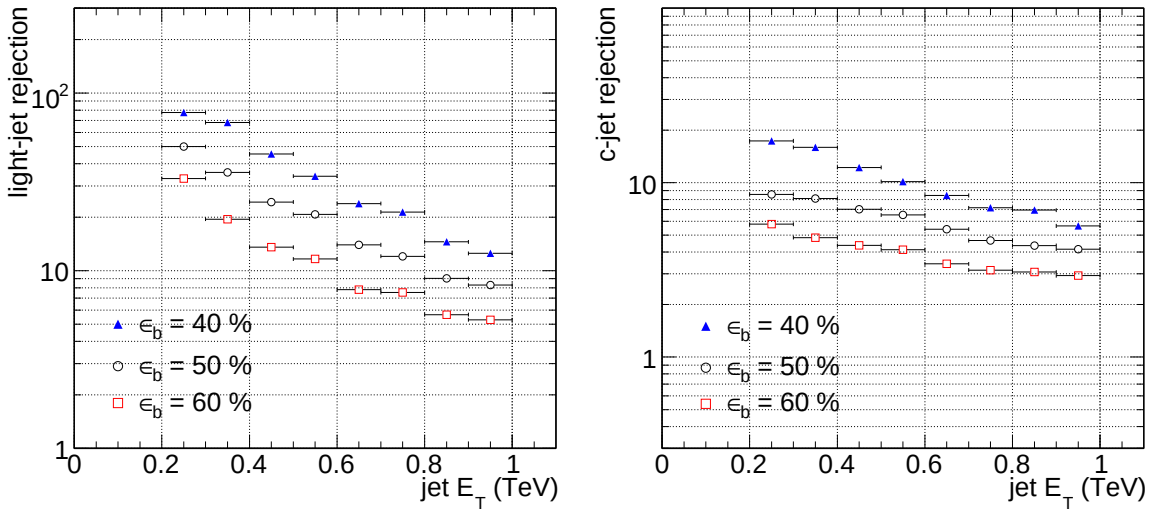

Figure 2: Light jet rejection (leftmost figure) and charm jet rejection (rightmost figure) versus jet transverse energy. The results correspond to the combined *SV1+IP3D* algorithm after a retuning for highly energetic jets. The three sets of markers represent three choices of the b-tagging efficiency.

The use of these retuned algorithm parameters leads to a considerable gain in performance (approximately a factor three in light jet rejection) in the interval 200 GeV $< E_T <$ 1 TeV. In the following, a single set of retuned parameters is used.

A further improvement in performance might be expected from a decidated *calibration* of the algorithms. In this context the term *calibration* refers to the determination of the set of probability density functions needed to determine the tagging likelihood. However, as no clear strategy for the determination of these PDFs for high p_T jets has been identified, in this analysis the default PDFs, tuned for low p_T jets, are used.

The b-tagging performance is traditionally reported in terms of rejection for u- and c-jets for a given b-tagging efficiency. The u- and c-jet rejection are defined as the inverse of the mistagging rate for u-jets and c-jets, respectively: $R_u = 1/\varepsilon_u$, $R_c = 1/\varepsilon_c$.

In figure 2 the b-tagging performance achieved for a high p_T jet sample is shown. For three values of the b-tagging efficiency - 60 %, 50 % and 40 % - the rejection for u-jets and charm jets are presented as a function of jet transverse energy [3)]. The most prominent feature is a steady degradation of the b-tagging performance as the jet momentum is increased.

[3)] To maintain constant efficiency over a large E_T interval the likelihood cut is adjusted for each bin.

5 Top *monojet* tagging performance

In this section, the potential of the ATLAS flavour tagging algorithms to identify jets that originate in the hadronic decay of high p_T top quarks is studied.

A sample of top *monojets* is obtained from the $Z_H \to t\bar{t}$ Monte Carlo sample. The *monojet* topology is selected by requiring that the top quark and the b-jet and W-boson produced in its decay are within a distance $\Delta R < 0.4$ of the reconstructed jet. The rejection of light jets is measured on a sample of u-quarks and c-quarks with a similar topology ($Z_H \to u\bar{u}$) to benchmark the performance of the algorithm. A discussion of the performance in the more realistic context of the QCD di-jet background (with realistic flavour content) is presented in section 6.

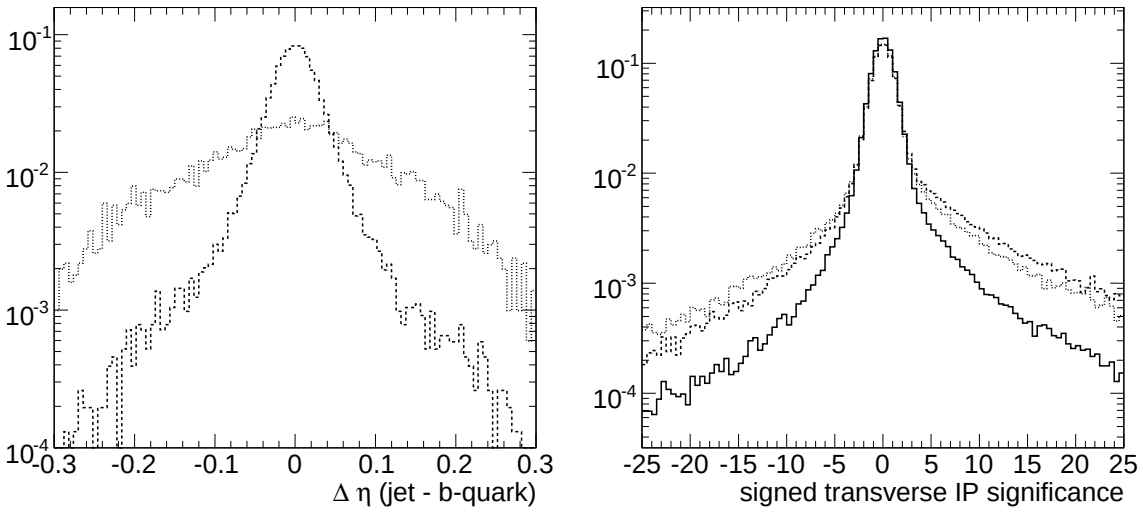

Figure 3: Leftmost figure: pseudo-rapidity difference between the reconstructed jet direction and the b-quark momentum. The dashed distribution corresponds to b-jets, while the dotted distribution represent hadronic top *monojets*. Rightmost figure: the signed impact parameter significance of all tracks inside light jets (continuous line), b-jets (dashed line) and hadronic top *monojets* (dotted line).

The presence of the jets from W-decay superposed on the b-jet distorts the performance of the tagging algorithms in several ways. In b-tagging algorithms the jet direction is normally identified with the B-hadron flight direction. This implicit assumption - used to determine the sign of the impact parameter - is a good approximation for b-jets over a wide kinematical range. In the case of hadronic top *monojets*, however, the jet direction is the weighted sum of the directions of the b-jet and the jets from W-decay, and this assumption is therefore expected to yield a poor estimate of the B-hadron direction. In the leftmost panel of figure 3 the difference in pseudo-rapidity between the b-quark and the reconstructed jet direction are shown for two samples. The dashed line corresponds to a high p_T b-jet sample ($Z_H \to b\bar{b}$), while the dotted lines corresponds to hadronic top *monojets* ($Z_H \to t\bar{t}$, where top quark, b-quark and W-boson are required to be within $\Delta R < 0.4$ of the reconstructed jet direction). As expected, the latter distribution is found to be much broader.

In the rightmost panel of figure 3 the signed impact parameter significance distribution is shown for light jets (continuous line), b-jets (dashed line) and top *monojets* (dotted line). The tail towards positive values in the significance distribution for b-jets is due to the large lifetime of B-hadrons. The much more symmetric distribution for top *monojets* reflects the large uncertainty on the B-hadron flight direction. In the ATLAS impact parameter based tagging algorithms tracks with negative significance do contribute

to the discriminating power, but with a much reduced weight. Therefore, the tagging performance is expected to be degraded by the larger uncertainty in B-hadron direction.

The larger mismatch between jet and B-hadron directions for top *monojets* limits the choice of the track-jet association cone size. Whereas for b-jets in the $Z_H \rightarrow b\bar{b}$ sample, 93 % of the tracks from B/D decay is contained within $\Delta R < 0.2$, in hadronic top *monojets*, the contained fraction is now reduced to 63 %.

The presence of tracks from W-decays in the hadronic top *monojet* contributes to the already quite dense environment of the b-jet. The number of reconstructed tracks in a cone with $\Delta R < 0.4$ around the jet direction is shown in the rightmost panel of figure 4.

In figures 5 the light jet rejection and charm jet rejection of the *SV1+IP3D* algorithm are given for three choices of the tagging efficiency. The data sample is divided in eight jet transverse energy bins from 200 GeV to 1 TeV.

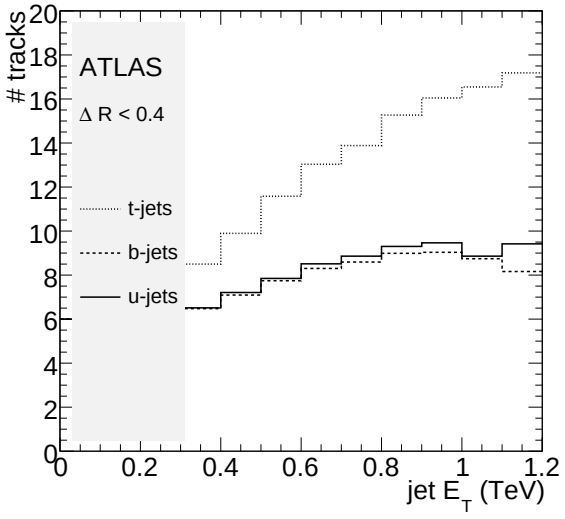

Figure 4: The number of reconstructed tracks ($p_T > 1$, $\Delta R_{jet-track} < 0.4$) versus jet p_T for u-jets (dashed), b-jets (dotted) and top quark with hadronic W decay (continuous line).

The potential to distinguish hadronic top *monojets* from u- and c-jets should be compared to the equivalent result for b-jets of figure 2. For comparable jet transverse energy and efficiency the rejection for light and c-quarks is significantly larger for b-jets than for hadronic top *monojets*. As discussed above, several effects related to the presence of the jets from W-decay are expected to lead to a degraded performance in top *monojets*.

In line with the above observation, the tagging performance for boosted top quarks where the W-boson decays leptonically should be less affected. And indeed, the performance on a sample of top *monojets* including all leptonic decay modes of the W (i.e. $W^{\pm} \rightarrow l\nu_l$, where l= $e^{\pm}$, $\mu^{\pm}$, $\tau^{\pm}$, including hadronic τ-decays) is found to be comparable to the results for b-jets in figure 2.

The light jet rejection of the algorithm depends strongly on the required efficiency. Across the jet p_T range the light jet rejection for a b-tagging efficiency of 60 % is approximately three times less than for an efficiency of 40 %. If higher signal efficiencies are required the rejection drops even further. For an efficiency of 70 % the light jet rejection is in the range between 8 (for jets in the p_T bin from 200 to 300 GeV) and 4 (for jet p_T between 900 GeV and 1 TeV).

Throughout the jet E_T range up to 1 TeV, hadronic top *monojets* can be distinguished on the basis of the lifetime signature of the embedded b-jet. For moderate tagging efficiency (30 %) a substantial rejection of light jets (greater than 30 up to jet transverse energy of 800 GeV) is achieved.

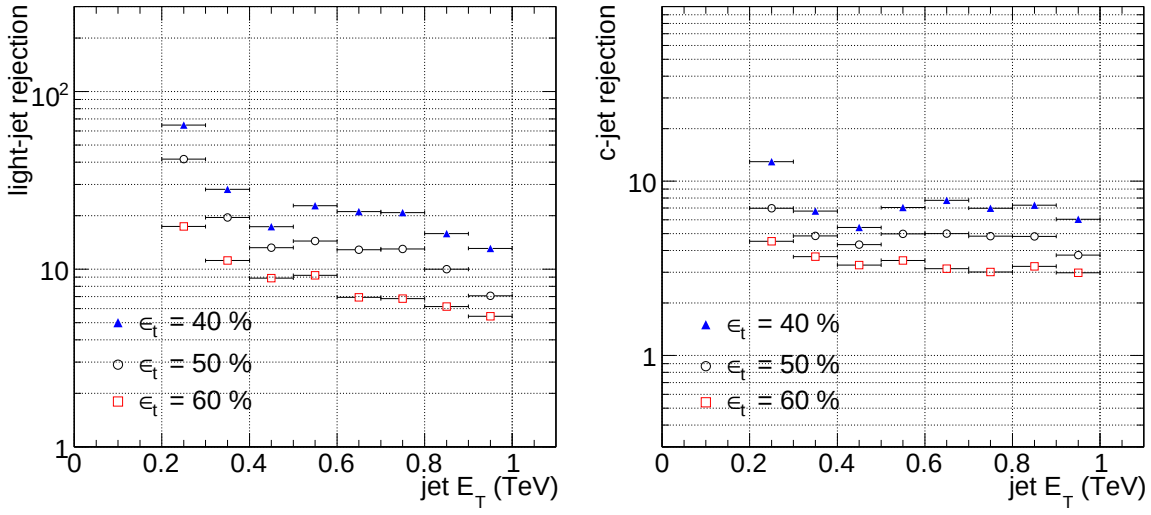

Figure 5: Light jet rejection (leftmost figure) and charm jet rejection (rightmost figure) of the combined *SV1+IP3D* algorithm versus jet transverse energy for three choices of the tagging efficiency for hadronic top *monojets*.

6 QCD background

In the previous section, the top *monojet* identification performance using lifetime based flavour tagging algorithms has been studied on topologies with a well-defined flavour content. To evaluate the potential and limitations of this method in a real physics analysis, the results are discussed here in the light of the flavour content of the QCD di-jet background.

The total QCD cross-section at the LHC is of the order of $1mb$ [4]. Direct production of heavy flavour (through the leading-order processes $q\bar{q} \to Q\bar{Q}$ and $gg \to Q\bar{Q}$, where Q designates heavy flavour, i.e. either c or b) is much less abundant: the direct production cross sections for $c\bar{c}$ and $b\bar{b}$ are nearly three orders of magnitude smaller than the inclusive di-jet cross-section [5]. The $t\bar{t}$ pair production cross section is approximately 800 pb.

However, the heavy flavour content in di-jet events is much higher than one would expect from the direct heavy flavour production cross-section. Heavy flavour production is enhanced strongly by heavy flavour production mechanisms known as flavour excitation [6] and gluon splitting [7]. While these are effects at $O(\alpha_s^3)$, they are numerically more important than the leading order processes [20].

The flavour fractions in the leading two jets in PYTHIA di-jet events are indicated in figure 6. Jet flavour is defined, as in the previous section, as the flavour of the heaviest quark found in a cone with $\Delta R < 0.4$ around the reconstructed jet axis.

In the rightmost panel of figure 6 the ratios of the different flavours are displayed as a function of jet

[4] The Pythia [19] cross-section for inclusive QCD (MSEL = 1) and a parton p_T cut-off of 20 GeV is 840 μb.

[5] Pythia returns a cross-section of several μb.

[6] In flavour excitation the heavy quarks are *present* in the proton parton density function.

[7] The dominant processes in inclusive high p_T di-jet production produce jets initiated by gluons. The relative contributions estimated using Pythia are: 56 % of the high p_T ($p_T > 560$) di-jet cross-section is due to the $qg \to qg$ process, while the processes $gg \to gg$ and $ff' \to ff'$ are of comparable magnitude, with 19 and 23 % respectively. The gluon has a considerable probability to split into a $c\bar{c}$ or $b\bar{b}$ pair. Thus, a large fraction of b-jets in inclusive di-jet samples contains two B-hadrons at small distance ΔR.

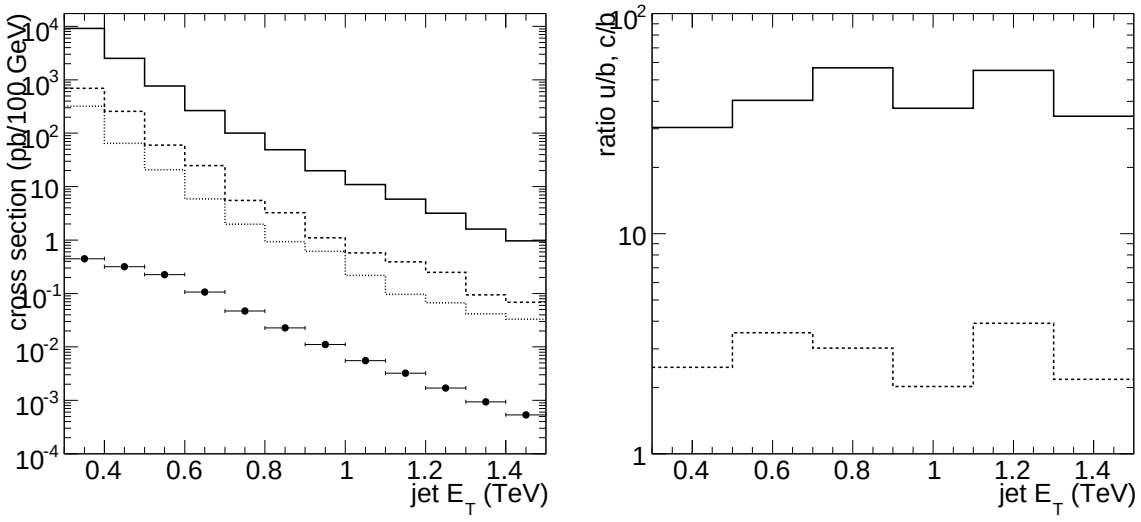

Figure 6: Leftmost figure: the flavour content of highly energetic QCD di-jet events. The continuous, dashed and dotted lines represent the abundance of light, charm and bottom jets, respectively. See text for the exact definitions. The production cross-section for top *monojets* is indicated by the round markers. These numbers include the branching ratio of $W \rightarrow q\bar{q}$ and the probability that the decay topology merges into a *mono-jet*. Rightmost figure: the ratio of light jets over b-jets (continuous line) and c-jets over b-jets (dashed line).

E_T. These ratios are found to be rather constant in the kinematic range studied here. The ratio of all jets to b-jets is found to be approximately 30, while the ratio of c to b-quarks is 2.5. These numbers indicate the maximal background reduction that can be achieved efficiently by flavour tagging. For a light-jet rejection beyond ~ 30 or a c-rejection beyond 2.5 the background will be dominated by the intrinsic bottom content of the QCD di-jet production, that is irreducible as far as flavour tagging algorithms are concerned.

The tagging performance results found in section 5 (reported in figure 5) show that the required light and charm-jet rejection can be obtained using the lifetime signature. For a light-jet rejection of 30, a tagging efficiency greater than 30 % is possible throughout the *monojet* transverse energy range of 200 to 800 GeV. The charm rejection is greater than 10 for the same range.

For comparison, the top *monojet* rate is indicated. No data sample is available in the CSC production that allows to determine the rate of Standard Model hadronic top *monojet* production [8)]. The points in figure 6 are therefore obtained from the $t\bar{t}$ cross-section - calculated using Pythia [19] in intervals of top p_T. The cross-section includes the branching fraction of $W \rightarrow q'\bar{q}$. Finally, the probability for a top quark of a given transverse momentum to yield a *monojet* - as defined in figure 1 - is taken into account.

The Standard Model hadronic top *monojet* production is approximately a factor 30 less abundant than b-jet production. The reduction of the b-jet background to the level of the irreducible $t\bar{t}$ background must be achieved by other means. In reference [9] the rejection of jets (including u, d, s, c, b and gluon jets) is investigated using a selection based on observables that reflect the substructure of the hadronic top *monojet*. For a fixed background rejection of 30, the top monojet efficiency ranges from over 40 % for moderate jet p_T (500 GeV $< p_T <$ 750 GeV) to greater than 20 % (1250 GeV $< p_T <$ 1500 GeV) [21].

[8)] The existing $t\bar{t}$ samples like 5200 or 5201 are either unbiased or preselect boosted tops with a moderate p_T threshold of 200 GeV. In either case, the statistics at high p_T is insufficient.

Top mono-jet selection on the basis of a combination of the lifetime and jet substructure signatures is a real possibility, albeit at a rather high cost in efficiency. Further improvements of the algorithms are actively being pursued.

It should be noted that the above discussion evaluates the worst case, where the signal selection relies only on the properties of a single hadronic top *monojet*. In practice, the top quarks are typically produced in association with other particles. Searches for neutral resonances into $t\bar{t}$ are performed using the semi-leptonic final state, where the selection benefits greatly from the presence of the lepton. In other cases the top quark may be produced in association with other particles (i.e. b-jets in the case of $W' \rightarrow tb$). Quite generally, the background rejection does not rely *only* on the ability of the ATLAS experiment to tag hadronic top *monojets*. The role of top *monojet* selection in the environment of a realistic analysis is currently being studied.

7 Summary and conclusion

Top quarks with a transverse momentum beyond 300 GeV have a considerable probability to be reconstructed as a single jet containing all decay products of the top quark. The isolation of hadronic top *monojets* from the high p_T di-jet background is an experimental challenge.

In this note, the potential of the lifetime signature of the B-hadron embedded in the hadronic top *monojet* is discussed. The ATLAS collaboration has developed a set of sophisticated flavour tagging algorithms based on the lifetime signature of B-hadrons. The potential of the combined *SV1+IP3D* algorithm to distinguish hadronic top *monojet* topologies from jets initiated by light, charmed or bottom quarks has been investigated.

The very small distance of the decay products of the W-decay to the b-jet affects the performance of the tagging algorithms in several ways. The reconstruction of the jet direction cannot be identified as readily with the B-hadron flight direction, leading to an increased probability to assign the wrong sign to the signed impact parameter. Moreover, the overlap with the hadronic W-decay adds tracks to the already dense environment. Comparing the hadronic top *monojet* tagging performance to that for b-jets of the same transverse energy, a significant degradation of the light and charm-jet rejection is indeed observed.

On the other hand, the potential of the lifetime signature is limited by the intrinsic flavour content in the QCD di-jet background. In high p_T di-jet events a charm quark is found within a cone of $\Delta R < 0.4$ of the jet direction for one out of ~ 12 jets. One out of ~ 30 jets contains a bottom quark.

Reduction of the di-jet background by a factor 30 (to the level of the b-jet content) is feasible using the lifetime signature of B-hadrons. The efficiency to identify top *monojets* is greater than 30 % for jet transverse energies up to 800 GeV.

Reduction of the remaining background to the level of the irreducible $t\bar{t}$ background must be achieved by other means, like those discussed in [9].

8 Acknowledgements

This work has been performed within the ATLAS Collaboration, making use of the physics analysis framework and tools which are the result of collaboration-wide efforts. The author would particularly like to thank L. Vacavant, C. Weiser and V. Kostyukhin of the ATLAS flavour tagging working group, and M. Bosman, G. Brooijmans, L. March, E. Ros for helpful discussions.

References

[1] B. Lillie, L. Randall and L.T. Wang, The bulk RS KK gluon at the LHC, JHEP 0709 (2007) 074, A.L. Fitzpatrick, J. Kaplan, L. Randall, L.T. Wang, Searching for the Kaluza-Klein Graviton in Bulk RS Models, JHEP 0709 (2007) 013.

[2] N. Arkani-Hamed, A. G. Cohen, E. Katz and A. E. Nelson, The Littlest Higgs, JHEP 0207, 034 (2002), N. Arkani-Hamed, A. G. Cohen, E. Katz, A. E. Nelson, T. Gregoire and J. G. Wacker, The minimal moose for a little Higgs, JHEP 0208, 021 (2002).

[3] Z. Chacko, H.-S. Goh and R. Harnik, The Twin Higgs: Natural electroweak breaking from mirror symmetry, Phys. Rev. Lett 96 (2006) 231802, H-S. Goh, S. Su, Phenomenology of The Left-Right Twin Higgs Model, Phys.Rev.D75 (2007) 075010

[4] L. March, E. Ros, B. Salvachua, Search for Kaluza-Klein excitations of the gluon in models with extra dimensions, ATL-PHYS-PUB-2006-002

[5] G. Azuelos et al., Exploring Little Higgs Models with ATLAS at the LHC, hep-ph/0402037; SN-ATLAS-2004-038, S. Gonzalez de la Hoz, L. March and E. Ros, Search for hadronic decays of Z_H and W_H in the Little Higgs model, ATL-PHYS-PUB-2006-003

[6] X. Miao et al., LHC studies of the left-right twin Higgs model, proceedings of the workshop for physics at TeV colliders, Les Houches, June 2007, M. Vos et al., Looking for signatures of the Left-Right Twin Higgs model with the ATLAS detector at the LHC, ATLAS note in preparation.

[7] S. Frixione and B. Webber, Matching NLO QCD computations and parton shower simulations, *JHEP* **0206** (2002) 029, P. N. S. Frixione and B. Webber, Matching NLO QCD and parton showers in heavy flavor production, *JHEP* **0308** (2003) 007,

[8] S. Bentvelsen, M. Cobal et al., Determination of the Top quark production cross section in ATLAS, A. Onofre, S. Tokar, Top quark properties, ATLAS CSC book, Top Physics chapter

[9] G. Brooijmans, High p_T hadronic top quark identification, Part I: Jet mass and Y-splitter, ATL-COM-PHYS-2008-001

[10] J. Butterworth et al., Y-splitter, an ATHENA tool for studying jet sub-structure, ATL-COM-PHYS-2007-077

[11] The ATLAS collaboration, b-tagging performance with ID misalignment, ATLAS CSC book, Flavour Tagging chapter

[12] The ATLAS collaboration, Reconstruction algorithms and performance, Detector level jet corrections, ATLAS CSC book, Jet Reconstruction chapte

[13] The ATLAS collaboration, The expected performance of the ATLAS inner detector, The ATLAS collaboration, The ATLAS Experiment at the CERN Large Hadron Collider, submitted to J. of Instr., in particular the section on the expected performance of the inner detector.

[14] L. Vacavant et al., b-Tagging Performance in ATLAS, ATLAS CSC book, Flavour Tagging chapter

[15] S. Corrard et al., b-tagging with DC1 data, ATL-PHYS-2004-006

[16] V. Kostyukhin, C. Weiser, Vertex reconstruction for b-tagging, ATLAS CSC book, Flavour Tagging chapter

[17] V. Kostyukhin, VkalVrt - a package for vertex reconstruction in ATLAS, ATL-PHYS-2003-031, V. Kostyukhin, Secondary vertex based b-tagging, ATL-PHYS-2003-033

[18] G. Piacquadio, C. Weiser ATL-PHYS-2008-???, G. Piacquadio, C. Weiser, Proc. CHEP 2007, Victoria, Canada

[19] T. Sjostrand, S. Mrenna, and P. Skands, PYTHIA 6.4 Physics and Manual *JHEP* **0605** (2006) 026.

[20] P. Nason, S.Dawson and R.K. Ellis, The total cross section for the production of heavy quarks in hadronic collissions, Nucl.Phys.B303 (1988) 607

[21] G. Brooijmans et al., private communciation.